Crytallography of Maraging Steel: Influence of Variant Selection.

Neuman Fontenele Viana [1];
Hamilton Ferreira Gomes de Abreu [1];

[1] *Department of Metallurgical Engineering and Materials,UFC, Fortaleza, Ceará, Brazil*
[1] *Corresponding author's email: neuman..fimat@gmail.com*

***Abstract*—In this work a study of the influence of variant selection on the crystallography after martensitic transformation in Maraging was studied. The study covered both the transformation under elastic deformation and also during plastic deformation. In Maraging steel, austenite becomes martensite at a temperature around 200ºC regardless of the cooling speed. To simulate the transformation during elastic deformation, a tensile test was performed in a furnace attached to a universal testing machine with an applied stress below the yield strength of the material. The specimen was heated to 850º C, the furnace was opened and the sample cooled in air under a constant stress. To study the influence of plastic deformation before transformation, samples were plastically deformed in a temperature above M_s (martensite start temperature), the external force acting on the sample was removed and the material was allowed to transform into martensite by cooling in air. Pole figures were measured by EBSD (Electron Back-Scatter Diffraction) in both conditions and compared with calculated pole figures assuming Patel-Cohen model and Taylor-Bishop-Hill model. The orientation of the parent austenite was obtained either by reversing the austenite by heating at 650 ° C and by using the mathematically reconstructed austenite grains. Results showed that Patel-Cohen model were more suitable to elastic deformation while Taylor-Bishop-Hill model was more appropriated to plastic deformation**.

***Index Terms*—Variant selection; Patel-Cohen; Taylor-Bishop-Hill**

I. INTRODUCTION

The maraging steel have mechanical strength and good ductility, a desirable combination, in addition, their characteristics allow studying the effect of deformation and applied stress separately, unlike austenitic.

For maraging steel there are few works available studying the influence of prior deformation in the variants selection and evolution of the microstructure.

The austenite to martensite transformation in ferrous alloys has been the subject of extensive research, a number of orientations relationships as KS[1], NW [2] and Bain[3] was proposed to connect the crystal orientations of the parent phase and product phase. Each of these assumes a correspondence between the planes and directions of lattices in the interface martensite and austenite, which leads to a limited number of possible variants after processing.

However, not all possible variants will always occur at the same intensity in each $\gamma \rightarrow \alpha$ transformation a preferential occurrence of a subset of variants is called the variants selection. it is known that many material properties such as strength, ductility, toughness, magnetic permeability, etc. are dependent on the texture.

Thus the understanding and control of the variants selection mechanism is reached, it should be possible to obtain only the variants that present the desired effects on the properties.

Many theories based on different selection criteria have been suggested to describe the variants selection in an attempt to predict transformation textures. Most criteria are based on the interaction between the plane habit and slip systems [4,5], or are related to the active slip systems of the prior deformation [6,7].

In this study, two models were used. Patel-Cohen[8,9] model, more suitable for elastic deformation, and Taylor-Bishop-Hill [10,11] model, used for plastic deformation. The two models were used in both situations, applied stress during the transformation and strain prior to transformation. The results were analyzed

II. EXPERIMENTAL

The maraging steel used was the 350 series, this steel was selected because its temperature at the beginning of the martensitic transformation around 200°C allows the study of the effect of applied stress separated from the effect of plastic deformation during the martensitic transformation. A plate of 2mm thickness was used to fabricate the specimens for tensile tests following ASTM E8-2003 for specimens of small size. The specimens were manufactured in workshop in the physics department at UFC. Figure 1 shows dimensions used.

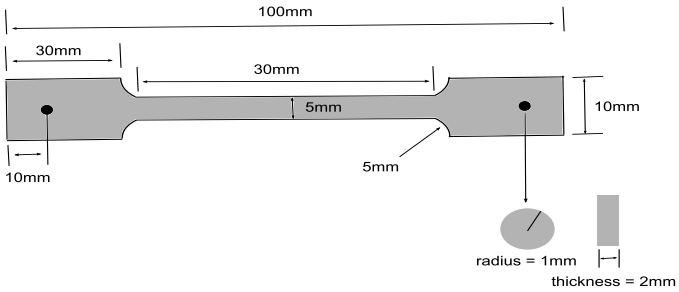

Figure 1 – Dimensions of the samples (out of scale).

From the chemical composition of the steel, the equilibrium diagram was calculated with the THERMO-CALC® program, with the phase diagram the temperature of 850°C was chosen for the austenitization of the specimens. Then the samples were heated in the oven coupled to mechanical testing machine EMIC DL 10000 located in DEMM at UFC until a temperature of 850ºC for 15 minutes to eliminate the martensite normally present in this material, the time was short so that there was no growth grains, and long enough to make the temperature uniform throughout the piece.

The M_s Temperature was determined by magnetic measurement, the M_s Temperature was around 200ºC. After austenitizing, the samples were cooled in the furnace to the temperature at which the tests were made, the experiments were conducted at temperatures of 400°C and 600°C above M_s Temperature, above this temperature the steel is austenitic. Levels of deformation were 0.1 of true strain for traction at each temperature. A test in which the sample was subjected to a stress below the yield stress at the temperature of 300°C was performed to study this effect. Finally, a sample without undergoing any mechanical effect was heated and cooled for comparison and was considered the reference sample. After the tests, the oven was opened at 300°C, the samples were removed for cooling air. Figure 2 summarizes the operations performed.

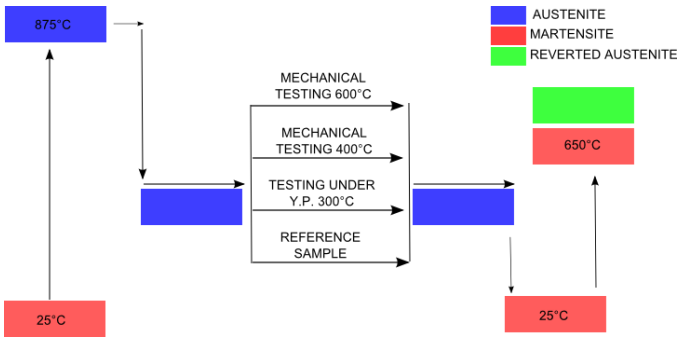

Figure 2 – Operations performed.

The samples were subjected to aging treatment at 650°C for 8 hours to obtain the reversed austenite, from which martensite variants would be obtained from established models. Assuming that the reversed austenite obtained is representative of the parent grain that formed martensite in that region.

The calculated pole figures by the models was compared to the measured pole figure in the region where the reversed austenite was generated. It should be noted that due to this treatment, a change may occur in the texture of the grains, alternatively to this treatment, and considering that obtaining prior austenite texture is important to the investigation of orientation relationships between austenite and the phase product, and aiming the study of the effect of prior deformation on the variant selection process, and since the maraging steel is martensitic at room temperature, ARPGE program [12] was used to recalculate the texture of the austenite from the martensite at room temperature. With the aged and recalculated measurements, MTex® a texture analysis toolbox of MATLAB® was used to acquire the orientation of the austenitic grains, and the measured and calculated pole figures.

The XRD patterns of the samples were obtained in the Philips XPRO diffractometer. The Co-K_α radiation was used in continuous mode with speed of 0.5° per minute. The scan started at 45° and ended in 105° to determine the presence of martensite and austenite phases. The measurements were performed in LACAM at UFC.

The presence of phases was confirmed using the XRD patterns in the X'Pert Highscore® program that uses the database PDF2. The peaks for austenite phase are approximately in the angles 51, 59 and 89. For the martensite phase, the peaks are found around 52, 77 and 99. Each peak corresponds to a diffraction plane.

The EBSD measurements were carried out in quanta FEG 450 in engineering and materials science department at the Gent University in Belgium. EBSD Image acquisition was performed using the TSL OIM software. The magnification was set at 3000x, and 0,2µm step size in accordance with the size of the martensite structure and the working distance was 11mm. The data were processed in MTex® program, where the ODF's and pole figures were obtained.

From the EBSD measurements, it was possible to obtain the orientations map of the austenite phase, allowing selecting regions, where small austenitic grains presented similar Euler angles, suggesting that any martensite formed in this region originated from a single austenite grain. The orientations map and Euler angles indicating the orientation of the austenite were obtained in MTex®.

In the chosen region, all orientations of the martensite grains were used to make the measured pole figures. During martensitic transformation, 24 variants have equal probability of occurring, but due to mechanical stress, some of these variants may occur preferentially, two models were used to predict what those variants, the Patel-Cohen model, suitable for the study of applied stress, and Taylor-Bishop-Hill model, more suitable for deformation. In both cases, the simulations were done from the Euler angles φ1, Φ and φ2 found in austenitic grains of selected regions.

In Patel-Cohen simulation, the crystal_habit_poly.f program developed by Saurabh Kundu [9] was used. This model calculates the variants with positive interaction energy. The generated file was imported into MTex®, and thus obtained the calculated poles figures.

In the Taylor-Hill Bishop model, the active slip systems of the orientation of the austenite was determined, each slip

system corresponds to an axis where the orientation of the austenite is rotated 90 degrees, resulting in 12 or 16 variants of martensite. The data were imported into MTex®, and obtained the calculated pole figures. The program used for the Taylor-Bishop-Hill model was Taylor.m, developed by the author of this work in the MATLAB programming language, using as reference the textbook [13] and the model developed by Viana et al [7].

III. MEMORY EFFECT OF TEXTURE

Simulations using the established models were performed, considering regions of the aged samples, where there were large amount of austenite with similar orientations. Whereas all martensite found in this region arose from the same austenite. The measured pole figure was obtained from the martensite, and the simulated pole figure was obtained from the austenite orientation. If the simulation considering all 24 variants from the reversed austenite for the sample without deformation and without applied tension during transformation match pole figure obtained from experimental martensite, there will be an indication that the austenite precipitates represents the parent grain, and indicate a memory effect of texture, then simulate the texture of martensite from these precipitates would be reasonable, and the reversed austenite have the same crystallographic texture of the original austenite.

Therefore, the first objective was to ensure that the parent austenite and the austenite reversed have the same crystallographic texture. FIG. 3 shows the scans made by X-ray diffraction for samples aged at 650 ° C for 2 hours, 4 hours and 8 hours.

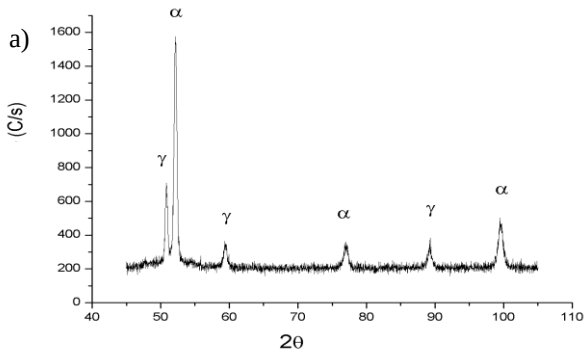

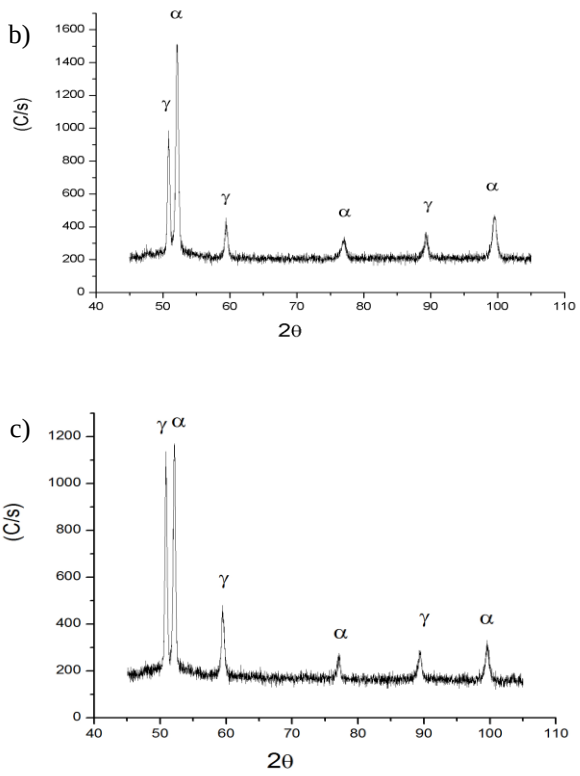

Figure 3 - X-ray scanning of the aged samples at 650°C during a) 2, b) 4 and c) 8 hours.

Comparing scans for different treatment times, it is evident that the amount of austenite increases with time. The Figure 4 show the ODF section φ2 = 45 degrees of the martensite phase.

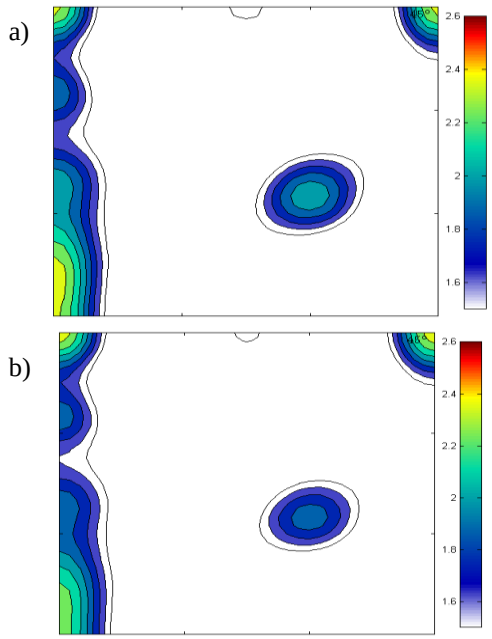

c)

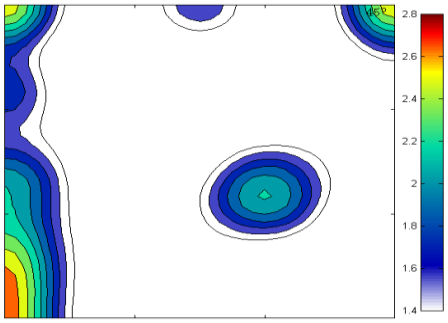

Figure 4 - ODF section φ_2 = 45º of the martensite phase of the aged samples at 650 ° C during a) 2, b) 4 and c) 8 hours.

Observing the ODF''s can be noted that the principal components of texture for all the aged samples are the rotate cube components (0, 0, 45) and (90, 0, 45), rotated goss (0, 90, 45) of α-fiber, and the component (60, 55, 45) in the γ-fiber. The rotated cube components and the α and γ-fiber textures are typical of deformation. The aged samples for 4 hours and 8 hours have larger peak intensity for the reversed austenite, but no significant change in crystallographic texture of martensite phase is observed, but only a slight increase in the intensity of rotated Goss component, then the amount of austenite formed does not influence the texture of the martensite phase.

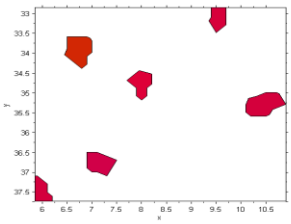

Figure 5 - orientations map of the austenite phase of the selected region.

Fig. 5 shows the orientation map of the austenite phase selected from a maraging sample aged for 8 hours at 650°C, cooled in air, with no applied tension and no deformation before martensitic transformation. The color of each point is associated with the local orientation. The red grain was selected, and it is suggested that all the martensite formed in this region has the same parent grain. The orientation of the austenite grain was determined by MTex® program and was represented by the set of Euler angles φ1 = 58.8, Φ = 45.1 and φ2 = 31.5. To perform the calculation of the orientations of the resulting martensite, a complete set of crystallographic data is needed. Unfortunately for the maraging steel, these data are not available. So the data that correspond to traditional twin {259}γ found in high carbon steels, Fe-Ni and Fe-Ni-C were used[14].

a)

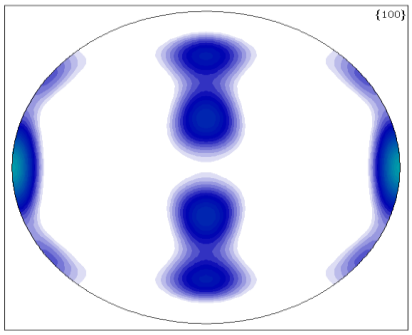

b)

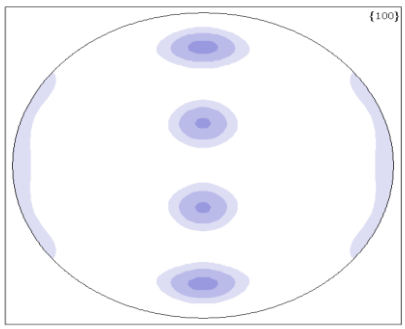

Figure 6 - Pole figures poles a) measured and b) calculated

Figure 6 shows calculated pole figure (100) using the PMTC (phenomenological theory of martensite crystallography) and assuming that all 24 variants are present, i.e. the variant selection is not acting, it was compared with the measured pole figure (100) for the same region. There is a very good correspondence between the measured and calculated pole figures. These results indicate the fact that the reversed austenite and the parent austenite have the same crystallographic texture. It is also evident that there is no variant selection in this transformation.

IV. SIMULATIONS OF AGED SAMPLES

Figure 7 shows the orientation map of the austenitic phase, the white area is composed of martensitic grains, from the martensitic grain, measured pole figures shown are obtained. The Euler angles of the austenitic grains are used to simulate the pole figures calculated by Patel-Cohen and Taylor-Bishop-Hill models. The measured and calculated pole figures are compared in Figures 8 to 10.

The range of the selected regions is given in microns. The pole figures (111) were chosen because they show the orientation of slip planes {111}, which are characteristic of FCC metals.

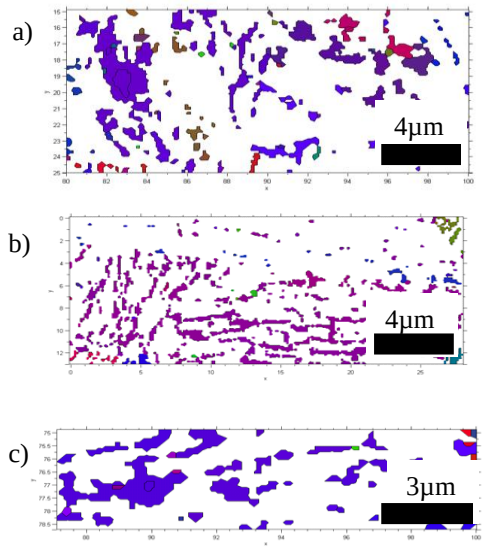

Figure 7 - Orientation maps of the austenite phase of the samples under a) applied stress, b) tested in 400ºC and c) 600ºC.

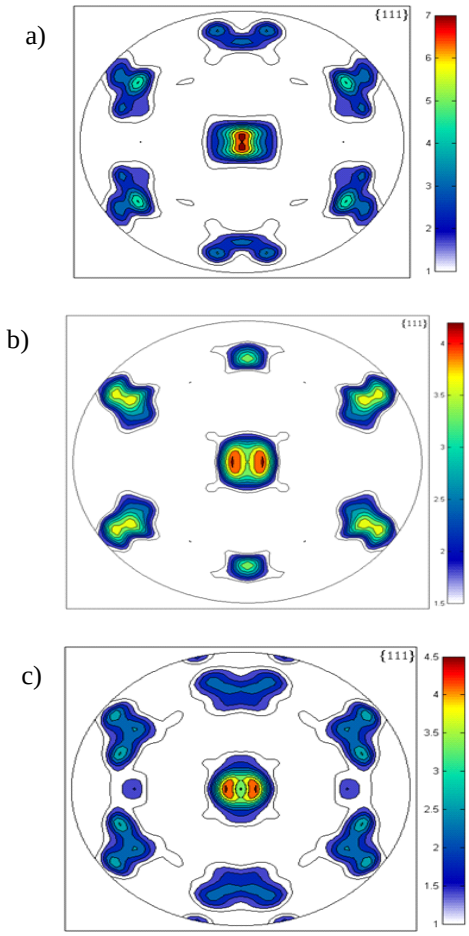

Figure 8 – a) Measured pole figure, calculated pole figure by the b) Patel-Cohen model and calculated pole figure by the c) Taylor-Bishop-Hill model of the sample under applied stress.

The sample subjected only to the elastic tractive force during the martensitic transformation is shown in Fig. 8. This sample showed a very good fit between the calculated pole figure and the measured, especially considering the pole figure calculated by Patel-Cohen. In the pole figure obtained by Taylor-Bishop-Hill, only a few variants with lower intensity arise in addition to those found in the measured pole figure, then the best fit was found for the model that considers the elastic conditions, as was expected, since this model examines the influence of applied tension during the transformation.

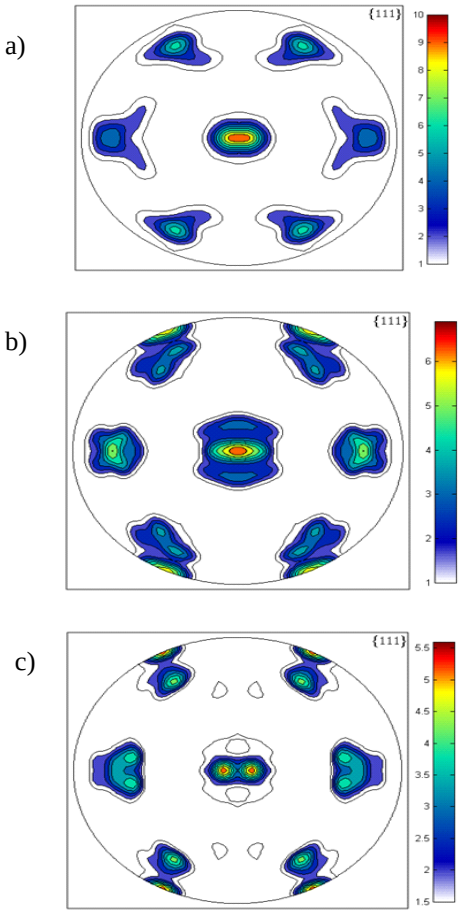

Figure 9 – a) Measured pole figure, calculated pole figure by the b) Patel-Cohen model and calculated pole figure by the c) Taylor-Bishop-Hill model of the sample tested in 400ºC.

Figure 9 compares the calculated pole figures and measured pole figures by EBSD for a grain belonging to the deformed sample by applying a tractive force at 400°C before to the martensitic transformation. Assuming that the applied deformation before transformation influences the level of variant selection, and therefore calculated pole figures was obtained by choosing only the variants with higher mechanical energy. Making a comparison between calculated Patel-Cohen and measured, it is observed that the model predicts all variants found experimentally, however some variants of moderate intensity, provided by the model are not present. In the Taylor-Hill-Bishop model, fit between the measured and calculated pole figure is better, where virtually all variants

were found. Although the fit is not perfect, because the Taylor-Hill-Bishop model is more suitable for larger deformations. Another reason for the worst adjustment would be the influence of thermal stress on the variant selection process because the samples were placed for cooling air.

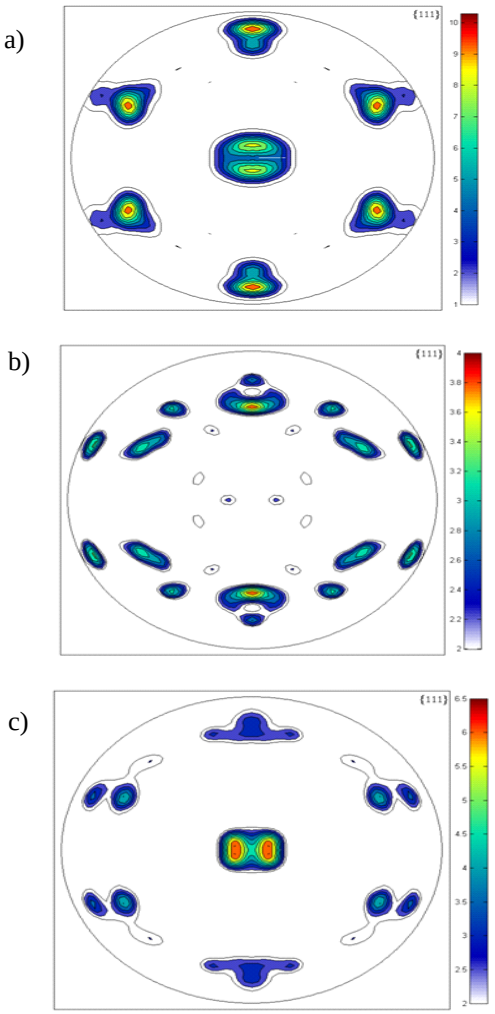

Figure 10 – a) Measured pole figure, calculated pole figure by the b) Patel-Cohen model and calculated pole figure by the c) Taylor-Bishop-Hill model of the sample tested in 400ºC.

For the sample deformed at 600°C, the fit is not good, when you consider the Patel-Cohen model, several variants do not coincide. In the Taylor-Bishop-Hill model, the fit is good and the calculated and measured poles figures are very similar, and most of the variants predicted by the model was found in measured pole figure, especially the higher intensity variants.

V. SIMULATIONS OF RECALCULATED BY ARPGE

For recalculated EBSD's the procedure for obtaining the austenite orientation was different from the one adopted for the aged samples. For this purpose, measurements without aging were obtained, in these samples there is no reverse austenite caused by aging, there is only the martensite phase, the austenite parent grains was recalculated from martensite by ARPGE program. In general, all measured region was recalculated, only not in some white regions. Austenitic grains used in the simulations were chosen in the recalculated measures, using full regions, and the Euler angles were taken. The measured pole figures were obtained in the equivalent region in experimental measurement, where the austenitic grain was chosen. Figure 11 show the orientation map of the selected regions of the austenite phase in µm, and Figures 12-14 show the measured and calculated pole figures (111).

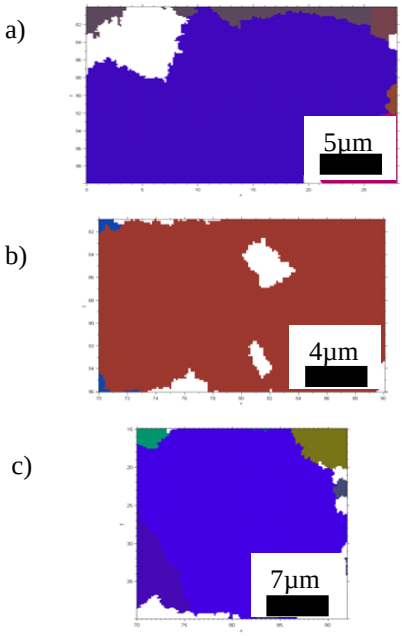

Figure 11 - Orientation maps of the austenite phase of the samples under a) applied stress, tested in b) 400ºC and c) 600ºC.

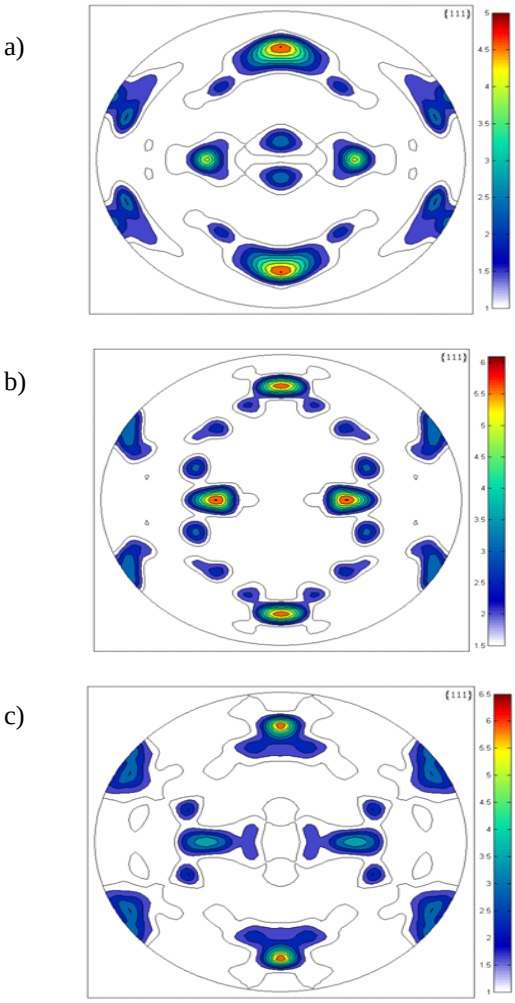

Figure 12 – a) Measured pole figure, calculated pole figure by the b) Patel-Cohen model and calculated pole figure by the c) Taylor-Bishop-Hill model of the sample under applied stress.

Figure 12 shows the simulated pole figure by Patel-Cohen, all higher intensity variants are found in the measured pole figure, except for two variants of intermediate intensity in the central region, the cause for this phenomenon can be the method of calculation for the reconstruction of the austenitic grains, this method uses Kurdjumov-Sachs relationship, and for reverse calculation the simulation by Patel-Cohen model is associated with PMTC (phenomenological theory of martensite crystallography)[15], because of this there is a deviation of the variants position of a few degrees. Comparing the measured and Taylor-Bishop-Hill calculated pole figure, it‘s seen that the fit in the variants position between the measured and calculated is good, although central variants do not appear clearly in the pole figure found by Patel-Cohen, despite in that case some contours are formed, perhaps because of the association between Taylor-Bishop-Hill model and KS orientation relationship in this simulation. The intensity found in the calculated pole figure by the model based on the elastic regime is closer than that considering the plastic model, so the simulation by Patel-Cohen showed the best result, as expected since this sample was only subjected to applied tension.

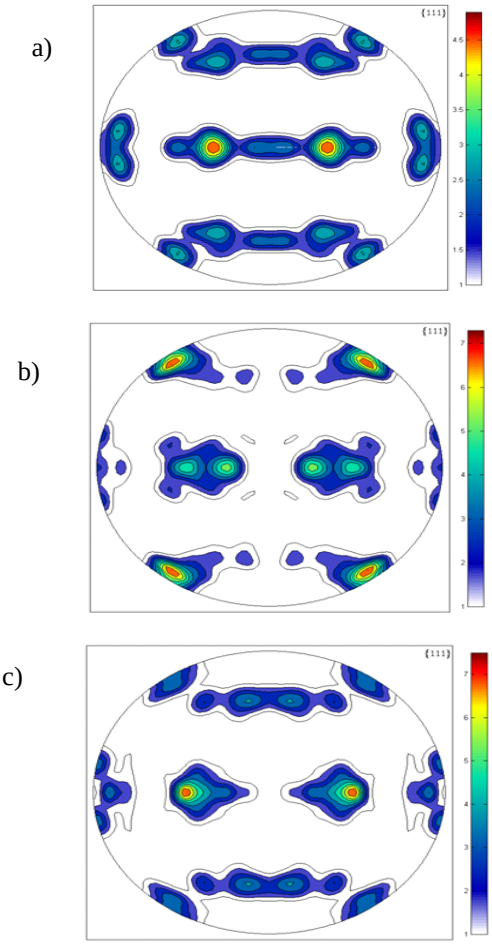

Figure 13 – a) Measured pole figure, calculated pole figure by the b) Patel-Cohen model and calculated pole figure by the c) Taylor-Bishop-Hill model of the sample tested in 400°C.

Figure 13 shows the measured and calculated pole figures. In the deformed sample at the temperature of 400°C, it is apparent that the best simulation was obtained by the program based on the Taylor-Bishop-Hill model, the calculated variants in simulated pole figure by this model are in the same place of the variants found in the measured pole figure. Clearly for the recalculated measurement, the difference between the pole figure calculated by Patel-Cohen model and the measured is much higher than that found for the sample that has undergone aging heat treatment for the emergence of reverse austenite, this can happen due to software designed to Patel-Cohen is associated with PMTC, while Kurdjmov-Sachs was used for reconstruction, generating an additional angular difference between calculated and measured variants. Another reason for the difference between the measured and calculated pole figures is the little applied plastic deformation, and simulations would be closer if larger deformations were applied as shown in previous works [7], but the EBSD technique is limited to get good quality measures for deformed

samples, therefore it was necessary to make measurements only for samples with low deformation.

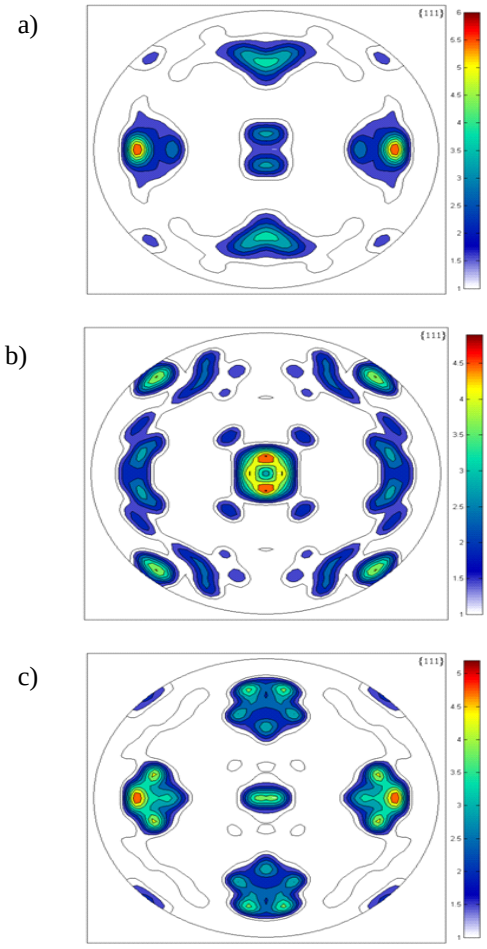

Figure 14 – a) Measured pole figure, calculated pole figure by the b) Patel-Cohen model and calculated pole figure by the c) Taylor-Bishop-Hill model of the sample tested in 600ºC.

The measured and calculated pole figures for the sample tested at 600°C are shown in figure 14, similar results to those obtained in the 400°C tests were found in simulations. In the calculations made by Patel-Cohen, many variants predicted by the model did not appear in measured and variants not predicted are present, a result that was expected. In the simulations using Taylor-Bishop-Hill, variants predicted by the model occupy the same region found in the measured pole figures, and variants of high intensity found in the measured pole figures correspond to the calculated, then the best fit simulation was obtained for the model that considers the plastic deformation, as expected. In general in the simulations obtained by Taylor-Bishop-Hill, higher intensity variants correspond to those found in measured pole figures, unlike what occurs in the pole figures obtained by Patel-Cohen, in which the variants of highest intensity generally are different from those found experimentally.

VI. CONCLUSION

In aged samples, the overall result of the simulation were as expected, the Patel-Cohen simulation in the sample under the applied stress was the best, although the intensity has not been perfectly adjusted, and the Taylor-Bishop-Hill simulation was the best for the samples deformed at different temperatures.

In samples recalculated the same phenomenon was observed, but the in sample under applied stress, the Patel-Cohen simulation was worse than in the previous case, because the reconstruction is done by a different model adopted in the Patel-Cohen simulation.

In general, considering tensile specimens and under applied stress, the Taylor-Bishop-Hill model showed better results.

ACKNOWLEDGEMENTS

The authors are grateful to the Prof. Leo Kestens and the Gent University of Belgium for EBSD measurements, Free University of Brussels, the CUD and CAPES for financial support and Cyril Cayron by recalculated measurements by ARPGE.

REFERENCES

[1] G., Kurdjmov, G. Sachs, “Über den Mechanismus der Stahlhärtung”. Zeitschrift für Physik, vol. 64, pp. 325-343,1930.
[2] Z. Nishiyama, Sci Rep Res Inst Tokohu Univ 1934-35;23:638.
[3] E. C. Bain , “Nature of Martensite”. Transactions of the metallurgical Society of AIME, vol. 70, p. 25, 1924.
[4] J.C. Brokos, E.R. Parker, Acta Mettallurgica, Vol.11,1963, p. 1291
[5] T.N. Durlu, J.W. Cristian, Acta Mettallurgica, Vol.27,1979, p. 663
[6] K. Haslam, “Deformation and recrystallization texture in metals and their industrial application”, Société de Metallurgie Nancy, 1975
[7] M.P. Butron Guillen, C.S. DaCosta Viana, J.J. Jonas, Met.Mat.Trans., Vol. 28, 1997, p. 1755
[8] J.R Patel, M. Cohen, “Criterion for the Action of Applied Stress in theMartensitic Transformation”, Acta Metallurgica, 1 (5), pp. 531-538. 1953.
[9] S. Kundu, “Transformation Strain and Crystallographic Texture in Steels.” [Ph.D. Thesis], University of Cambridge, Cambridge, 2007.
[10] J.F. Bishop, R. Hill. Philos Mag 1951;42:414.
[11] J.F. Bishop, R. Hill. Philos Mag 1951;42:1298.
[12] C. Cayron, B. Artaud, L. Briottet, 2006. Mater. Charact. 57, 386-401.
[13] W.F. Hosford,, “The Mechanics of Crystals and Textured Polycrystals”, Oxford University Press, New York, 1993
[14] P. M. Kelly, ISI Special Rep 1964;86:146.
[15] H. K. D. H Bhadeshia, “Worked Examples in the Geometry of Crystals”, Intistute of Materials, London, 2001.